

# Performance Evaluation of Above-Ground Weighbridge using Finite Element Analysis

<sup>1</sup>Dhananjay Singh, <sup>2</sup>Mr. Mousam Sharma

<sup>1</sup>Dhananjay Singh, M.Tech Scholar, Department of Mechanical Engineering, SISTec, Bhopal (M.P.), Bhopal (MP), India.

<sup>2</sup>Mr. Mousam Sharma, Assistant Prof., Department of Mechanical Engineering, SISTec, Bhopal (M.P.)

Email <sup>1</sup> [mousamsharma@sistec.ac.in](mailto:mousamsharma@sistec.ac.in)

\* Corresponding Author: Dhananjay Singh

**Abstract:** A weighbridge is a critical tool in managing vehicle overloading and preventing premature pavement deterioration. The cost-effectiveness of a weighbridge depends on its ability to save more pavement costs than its operational expenses. Various external factors, such as heavy-vehicle traffic, axle load distribution, weighbridge capital and maintenance costs, revenue from fines, and road repair expenses, influence the overall cost. This study presents the working principle of weighbridges, which utilize load cells with strain gauges and digital monitors to measure vehicle weights. The gross weight, including the truck and payload, is measured initially, and the payload weight is then calculated by subtracting the truck's weight. Different types and characteristics of weighbridges, as recognized by international metrology standards, are discussed. The advantages of weighbridge use include enhanced productivity, immediate identification of overloaded vehicles, streamlined compliance enforcement, automated data recording, and cost-effectiveness. The primary objective of this work is to design and optimize an above-ground weighbridge using finite element analysis. The study outlines the goals, methodology, and results of the structural analysis performed on four different proposed weighbridge designs. The structural behavior, deformations, stresses, and equivalent strains of these designs are evaluated, leading to the selection of the most optimal design for an above-ground weighbridge.

**Keywords:** Weighbridge, vehicle overloading, pavement deterioration, cost-effectiveness, load cells, strain gauges, finite element analysis, structural analysis, design optimization.

## I. INTRODUCTION

A weighbridge is a tool used to manage vehicle overloading and halt the premature deterioration of pavement. A weighbridge must be cost-effective if it can save more pavement than it costs to operate. The cost of the weighbridge is influenced by external factors like the magnitude of heavy-vehicle traffic, the distribution of axle loads, the capital and maintenance costs of the weighbridge, revenue from fines, and the frequency and cost of road repair. [1] A set of scales used to weigh big objects is called a weighbridge or truckscale. The producer of weighbridges mounts a set of scales on a concrete surface. It has a digital or electronic monitor that shows the vehicle's weight being weighed.

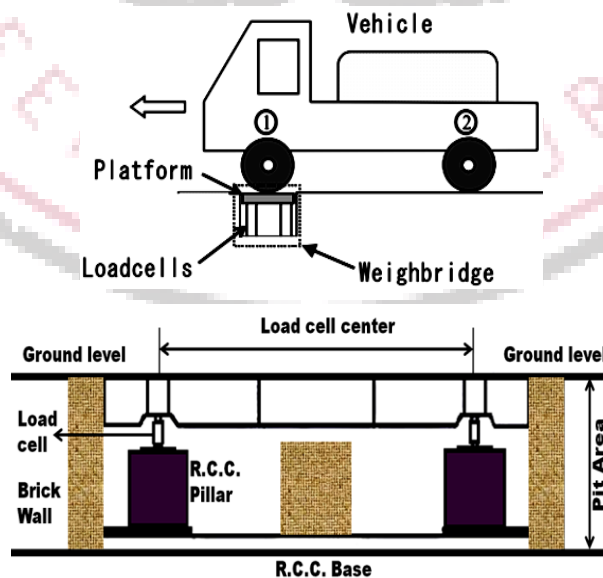


Figure 1. Weighbridge Structure

### A. Working principle of Weighbridge

On load cells, the complete Steel platform is mounted. One or more strain gauges are attached to or incorporated into each load cell, which is made of a robust material like steel or concrete. A wire that carries a mild electric current makes up a strain gauge. The load cell strain gauge's wire is adjusted or slightly compressed as the cell is squeezed underweight. A difference in the wire's resistance to current flowing through it is caused by the change in the wire. Each load cell sends an analogue signal to the junction box. Junction boxes aggregate the signals from various load cells and send the total signal to the controller of the weighbridge. The controller uses an analogue to digital converter to digitize the junction box signal, and the weight is shown on an LED display. Driving the truck first onto the weighbridge allows for the measurement of the gross weight, which is the total weight of the payload, including the truck. The total weight must then be removed from the gross weight to get the payload's weight. [2].

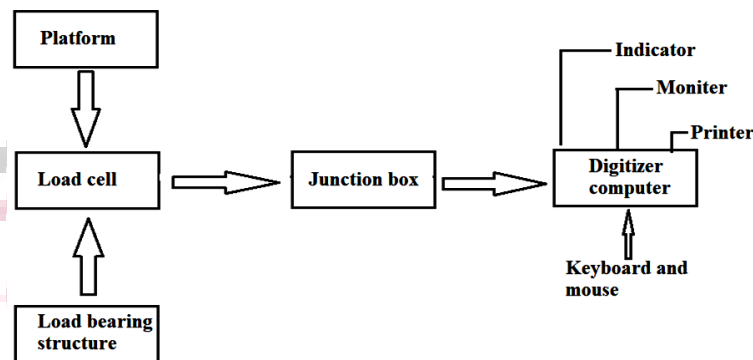


Figure 2. Working principle of weighbridge

### B. Types and Characteristics of Weighbridges

In principle, any of the following types of vehicle-weighing systems are officially recognized by the International Organization of Legal Metrology (Organisation International de Metrologies Legal, OIML) for vehicle weighing purposes.

Table 1 OIML Approved Types of Weighing Systems

Type of Weighing System	Vehicle Element Weighed
Static- fixed	Total weight (GCM)
Static or dynamic: low speed – fixed	Single, tandem, or tridem axle
Static or dynamic: low speed – mobile	Single, tandem, or tridem axle

OIML-approved weighing material guarantees accurate measurement results and reliability throughout time. Such certification ensures robustness and solidity standards, e.g., the weighing platform must be able to bear the breaking of a 50 tone axle at 30 km/h without being damaged in any way. This requires that the materials used in the construction of the weighbridge have undergone a series of tests which comply with OIML standards. Although various types of OIML-approved weighing systems may be used for vehicle weighing purposes, they exhibit varying characteristics and a careful choice must be made in relation to the main purpose of weighing the vehicle.

### C. The Advantages of Weighbridges

These are four universal benefits of using weighbridges [3].

- Firstly, they enhance productivity. Utilizing a weighbridge is an efficient way of checking the weight. The process is quick, which stops drivers from waiting around unnecessarily.
- They instantly notify you if a vehicle is overloaded. Weighbridges prevent overloaded cars from driving onto the roads; you are immediately protected from potential infringements. Weighbridges help to enforce compliance with the rules.
- With a good weighbridge, you get access to extensive reporting as data is recorded automatically and stored securely. This could be useful if needed to be referred to at a later date.
- Lastly, they're cost-effective. Implementing a weighbridge has minimal expenses.

## II.LITERATURE REVIEW

Li, J., et al. (2020) [4] As an important preventive and remedial application of lost circulation, the optimization of lost circulation materials (LCMs) has become a crucial problem. In order to optimize the design of LCMs, the mechanism of bridging was studied. Based on the theory of solid-liquid flow, a coupled Computational Fluid Dynamics (CFD) - Discrete Element Method (DEM) model was introduced to accurately simulate the dynamic bridging process of plugging particles. The critical bridging concentration is more sensitive to the ratio of inlet size to outlet size ( $R_{io}$ ) with a higher ratio of outlet size to particle size ( $R_o$ ). For a small outlet size ( $R_o \leq 2.5$ ), the bridging state can be observed obviously because the large

particles are dominant. When the outlet size is larger ( $Ro > 3$ ), the stable plugging zone is hard to form because the dense state increases the risk of friction failure. The hindering effect of gravity on the trajectory of particles will be more significant when the fracture extension direction is perpendicular to the gravity direction.

**Shu, J., et al. (2019) [5]** A Multi-Level Assessment Strategy has previously been proposed and proved feasible for structural analysis of existing RC slabs. In this paper, the Multi-Level Assessment Strategy, which focuses on sophisticated structural analysis, was used to investigate the load-carrying capacity and structural behaviour of a composite bridge with an RC bridge deck slab subjected to a concentrated load. In addition to more sophisticated structural analysis, improved knowledge content about the structure and more advanced models for uncertainty consideration were also incorporated in a systematic way for higher levels of assessment. Furthermore, a decision support system was adopted, in which the cost for different alternatives regarding if and how the assessment should be enhanced with respect to model sophistication, knowledge content and modeling uncertainty were compared in a systematic way. The results show not only that the load-carrying capacity and the structural behaviour can be assessed with different level of detailing, but also that the cost for each level of assessment can be evaluated with a decision support system, facilitating more sustainable management of infrastructure.

**Hassoun, M., & Fatahi, B (2019). [6]** An external restraining system which is anchoring the bridge superstructure to the embankment backfill is proposed in this study for the seismic protection of isolated bridges. The restraining system is employed to reduce the seismic demands of the bridge deck by utilizing the otherwise inactive ground behind the abutment back-walls. The system can be described as fastening the bridge end-diaphragms to the rocky strata that lie beneath the abutment backfill. The anchoring is achieved through a series of steel strands grouted to the rock to achieve a strong anchoring capacity. Indeed, the proposed anchor is flexible enough to allow the thermal, creep and shrinkage serviceability movements of the deck. A parametric study conducted in this paper shows that the ground anchor external restraining system is truly effective in reducing the seismic demands of the bridge deck.

**Mokrani, B., et al. (2017) [7]** A relatively common, cost-effective, and reliable method of reducing the dynamic response of civil engineering structures is the use of Tuned Mass Dampers (TMDs). However, the number of TMDs used in their classical implementation equals the number of critical modes. This study examines a TMD with two degrees of freedom that aims to concurrently mitigate a bridge deck's bending and torsion modes. Both the bending mode and the torsion mode can be modified independently using the system parameters. The investigation is carried both numerically and experimentally on a suspension bridge laboratory mock-up.

**Cantero, D., et al. (2017) [8]** This article describes an experimental programmer that aimed to measure the change in bridge modal characteristics during a vehicle's passage. It examines changes in the appearance of the vibration modes as well as frequency shifts brought on by various vehicle locations. By traversing vehicles or trucks that were temporarily stationed on the bridge, two distinct bridges were instrumented and loaded. An output-only method and a novel application of the continuous wavelet transform, which is reported here for the first time, were used to analyze the measurements. The results of the investigation show that there are extra frequencies, considerable frequency shifts, and modifications in the modes of vibration. A simplified numerical model is used to theoretically study these occurrences. This paper offers an interpretation of vehicle-bridge interaction of two particular case studies. The results clearly show that the modal properties of the vehicle and bridge do change with varying vehicle position.

**Bistak, M., et al. (2017) [9]** The design of the about-ground weighbridge is presented in this publication. The usage of this instrument is required in order to reassess the weight of the trucks utilised to convey the gathered steel waste to the collection yard. To ensure that the vehicles do not exceed the maximum weight allowed by law for the transportation of products by road, weighbridges are used wherever vehicles must be weighed. The use of advanced CAD/CAE systems in the design and optimisation process enabled a number of changes to be made to the steel structure, resulting in an ergonomic installation, weight reduction, increased strength, and higher stiffness of the structure under load.

### III. OBJECTIVES

The primary goal of the current work is to use finite element analysis to design and optimise the performance of an above-ground weighbridge. The current work has the following goals.

1. To create the different three dimensional CAD model of weighbridge using different section of the profile.
2. To perform the structure analysis on created three dimensional CAD model of weighbridge in order to investigate the total deformation, directional deformation, equivalent stress & equivalent strain.
3. Compare the results obtained from the structure analysis and suggest better design of the above-ground weighbridge.

### IV. METHODOLOGY

The model of the load cell is represented as a Mass Spring Damper (MSD) system as shown in figure 4.1, where  $m$  is the mass of the desired item subjected to the load cell.  $M$  is the equivalent mass of the load cell that is attached to a mass-less spring with spring constant  $k$ .

As the load is applied to the load cell, a counteracting force produced by the spring due to an offset  $x$  from equilibrium is defined by Hooke's law.

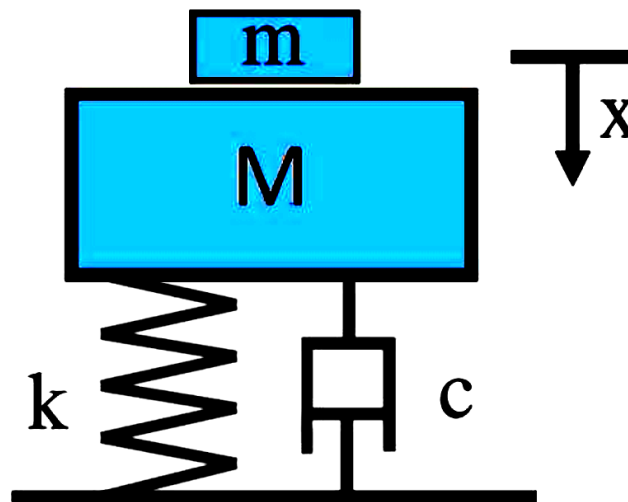


Figure 3 Mass Spring Damper System

$$f_s = -kx \quad (4.1)$$

This would be sufficient to model the load cell in a static equilibrium, but in analysing the dynamic characteristics, it is important to take into account the damping. Viscous damping is assumed, where the damping force is proportional to the velocity:

$$f_D = -c \frac{dx}{dt} \quad (4.2)$$

Where:

$f_D$  Damping force

$c$  = damping coefficient

By using Newton's second law the following differential equation is obtained:

$$(M + m) \frac{dx^2}{dt^2} = -c \frac{dx}{dt} - kx + mg + Mg \quad (4.3)$$

The above equation can be used in cases where the deflection is from a steady state that is not solely by the mass of the load cell, i.e.  $m \neq 0$ .

Where

$g$  = average acceleration produced by Earth's gravity ( $9.81 \text{ m/s}^2$ )

The solution of the above equation can be obtained from

#### A. ANSYS Capabilities

In FEM (finite element analysis) ANSYS software is used that helps engineers for performing the following works:

- To build computer prototype, components, transfer CAD model structures in a system products.
- Enhances the profile of structural member with shape optimization.
- To study stress levels, temperature distributions.
- To reduce production costs design should be optimized in early development process.
- Testing of prototypes is done in normal condition where it otherwise would be undesirable or impossible (for example, biomedical applications).

#### B. Algorithm used for Finite Element analysis

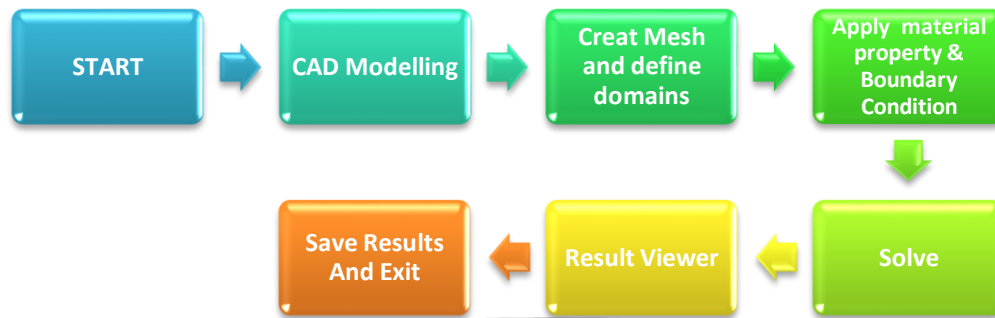


**Figure 4.** Algorithm used for Finite Element analysis

**Table 4.1** Parameter used to model the weighbridge

Parameter	Value
Measuring range of the weight	Maximum 40 tonnes
Dimensions of the weight (WxLxH)	4x10x0,5 [m]
The base of the bridge profile	IPE 220
Weighing surface size W x L	3 x 6.53 m
Structure variant	Steel
Operating temperature limits	-50 °C to +80 °C
The surface load on front axle 2x F	30000 N
The surface load on rear axle 4x F	50000 N
Fixed support	bearing surfaces both side of the weighbridge
gravitational acceleration g	9,8066 m.s-2
Placement	Above-ground

### C. CAD Geometry of design-1

The three dimensional CAD model of design-1 weighbridge has been created in design modular of ANSYS workbench with the dimensions of length of 4m x 10m x 0.5m and consists the ladder frame of IPE 220 profile with depth 220 mm, width 110 mm web thickn tion of web is 177.6 mm as shown in figure.ess is 5.9 mm, flange thickness 9.2, inner depth between flange 201.6 mm, root fillet radius 12 mm & depth of straight por

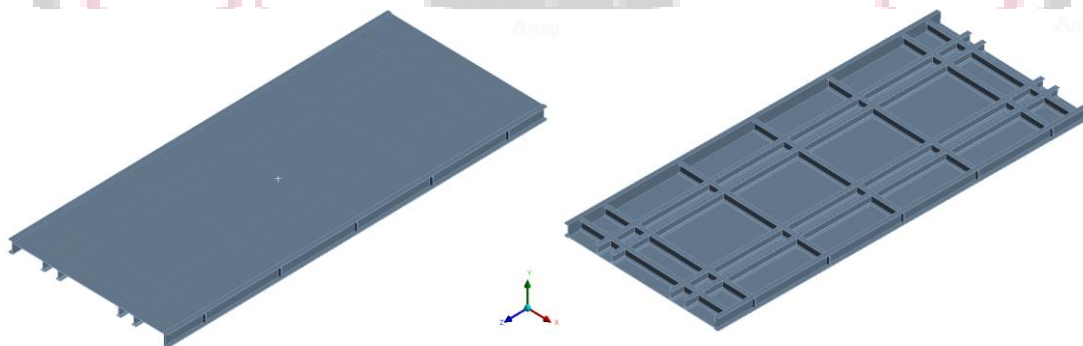


**Figure 4.** CAD geometry of design-1 weighbridge

**Meshing of design-1:** After the creation of CAD model, the next step is meshing, meshing is a critical operation in which CAD model is divided into small pieces of elements or discretization of CAD geometry. In the present work total, no. of nodes is 1103332 and the total number of elements is 513336 having tetrahedral & hexahedral elements as shown in figure.

**CAD Geometry of design-2:** The three dimensional CAD model of weighbridge proposed design-2 has been created in design modular of ANSYS workbench with the dimensions of length of 3m x 10m x 0.5m and the base of the bridge profile is box type (100 mm x 100 mm 8 mm) as shown in figure.



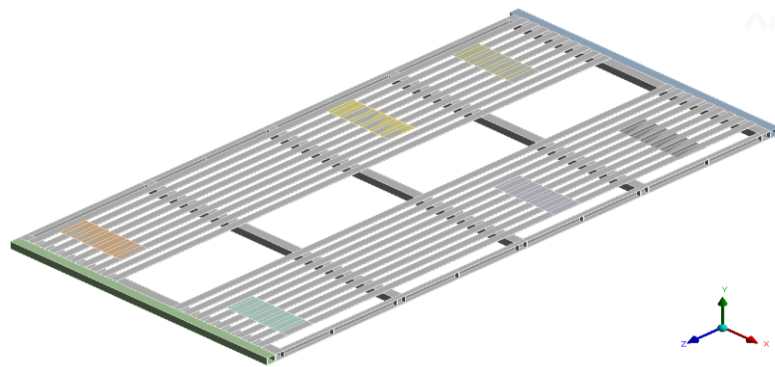


**Figure 6.** CAD geometry of weighbridge proposed design-2

**CAD Geometry of design-3:** The three dimensional CAD model of weighbridge proposed design-3 has been created in design modular of ANSYS workbench with the dimensions of length of 3m x 16.92m x 0.5m and the base of the bridge profile is box type (100 mm x 100 mm 8 mm) as shown in figure.

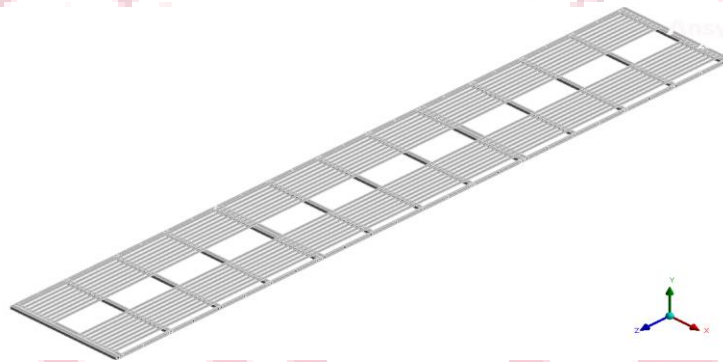


**Figure 7.** CAD geometry of weighbridge proposed design-3

**CAD Geometry of design-4:** The three dimensional CAD model of weighbridge proposed design-4 has been created in design modular of ANSYS workbench with the dimensions of length of 3m x 16.92m x 0.5m and consists the ladder frame of IPE 220 profile with depth 220 mm, width 110 mm web thickness is 5.9 mm, flange thickness 9.2, inner depth between flange 201.6 mm, root fillet radius 12 mm & depth of straight portion of web is 177.6 mm as shown in figure.

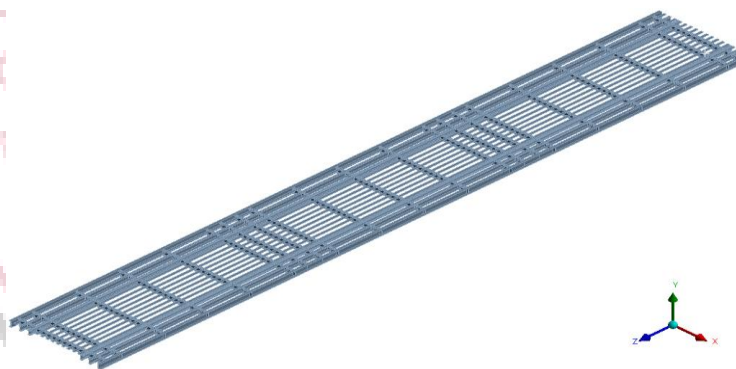


**Figure 8.** CAD geometry of weighbridge proposed design-4

#### **D. Grid independent Test**

Grid independent is associated with the accuracy of numerical results, the grid is independent directly influences the truncation error or even the rationality of numerical results. When considering grid-independent test, a very dense grid can avoid this problem but the calculation resource may be wasted unnecessarily. In practice, we usually increase the grid resolution according to a certain ratio and then compare the results of two neighborhood results. If the results tend towards identical the grid can be considered as grid-independent. Such strategy can utilize computational resource most efficiently as well as obtain reasonable results.

In the present work finite element analysis have been conducted on the above-ground weighbridge with the dimensions of length of 4m x 10m x 0.5m and consists the ladder frame of IPE 220 profile to check the stresses and deformation.

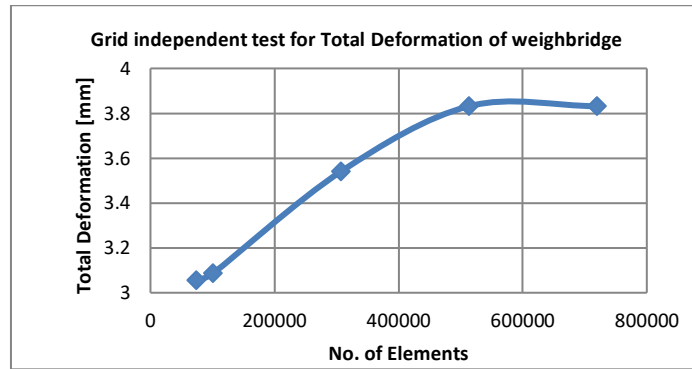


Figure 9. Grid independent test for total deformation

V. RESULTS AND DISCUSSION

The main objective of the present work is to design and optimization of above-ground weighbridge using finite element analysis. For that there are total four design of the weighbridge have been used to perform structural analysis in order to check the total deformation, Directional deformation, equivalent stress & total equivalent strain or permanent deformation. For the structural analysis consider the static weighing fully loaded vehicle up to 26t, there are total six surfaces are in contact between the bridge and wheels where two of front axle and other four are with the rear axle of the vehicle. The surfaces are loaded with forces  $2 \times F = 30000$  N for the front axle and  $4 \times F = 50000$  N for the rear axle, the fixed support has been applied to the bearing surfaces both side of the weighbridge while the gravitational acceleration of  $9.81$  m/s<sup>2</sup> placed at the full structure of the weighbridge.

A. Structural Analysis of the Above-Ground Weighbridge for Design-1

After performing structure analysis of the weighbridge for design-1 at forces of 30000 N at the front axle and 50000 N at the rear axle applied in vertical direction, the total deformation of 3.83 mm has been observed at the rear axle of the weighbridge as shown in figure.

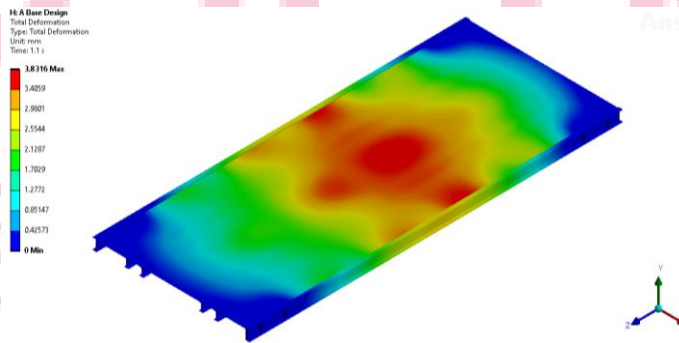


Figure 10. Total deformation of weighbridge for design-1

After performing structure analysis of the weighbridge for design-1 at forces of 30000 N at the front axle and 50000 N at the rear axle applied in vertical direction, the Directional deformation along the Y-axis of 3.51 mm in downward direction has been observed at rear axle of the weighbridge as shown in figure.

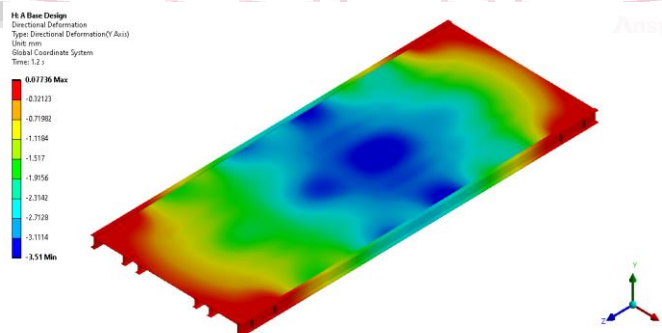
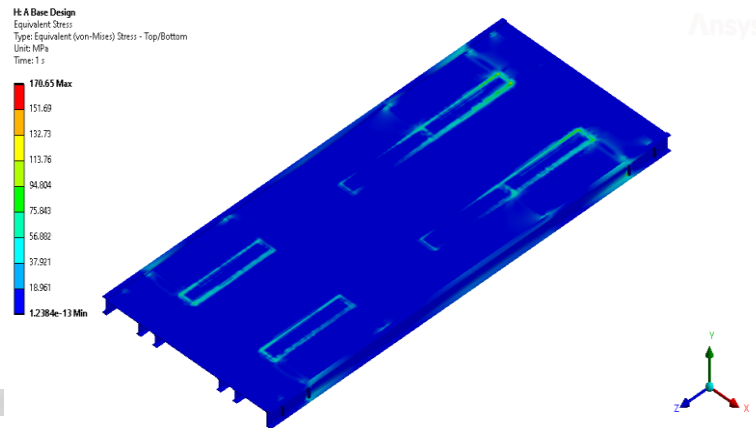


Figure 11. Directional deformation along Y-axis of weighbridge for design-1

After performing structure analysis of the weighbridge for design-1 at forces of 30000 N at the front axle and 50000 N at the rear axle applied in vertical direction, the maximum equivalent stress of 170.65 MPa has been observed at the loaded portion of the front & rear axle of the weighbridge as shown in figure.



**Figure 12.** Equivalent stress of weighbridge for design-1

After performing structure analysis of the weighbridge for design-1 at forces of 30000 N at the front axle and 50000 N at the rear axle applied in vertical direction, the equivalent total strain of 0.000144 mm/mm (0.0978%) has been observed at the loaded portion of the front & rear axle of the weighbridge as shown in figure.

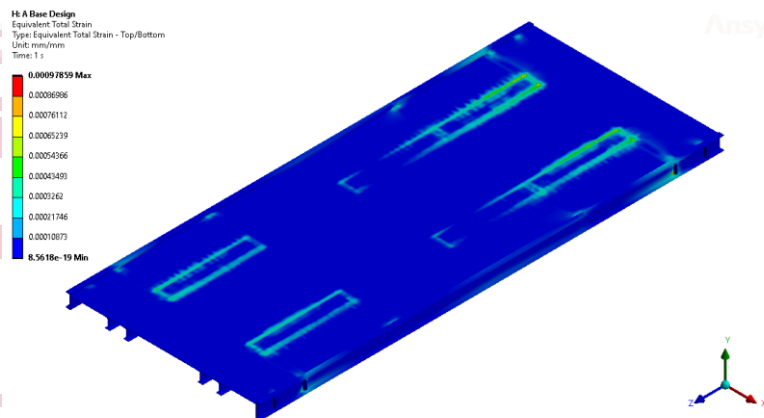


**Figure 13.** Equivalent strain of weighbridge for design-1

**Direction Deformation along the Contact Length of the Weighbridge at the Rear Axle for Design-1**

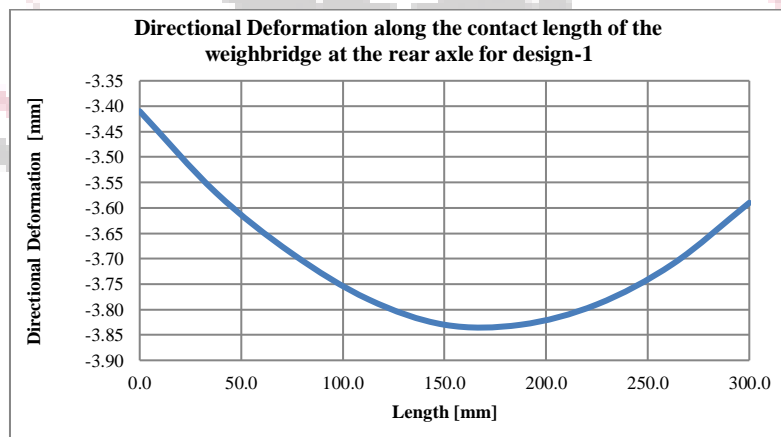


**Figure 14.** Directional deformation along the contact length of the weighbridge at the rear axle for design-1

From the above graph it has been observed that the directional deformation along the contact length of the weighbridge at the rear axle for design-1 increasing gradually from 3.41 mm to 3.83 mm and then decreasing up to 3.59 mm as shown in figure.



**Equivalent Stress along the Length of the Weighbridge at the Rear Axle for Design-1**

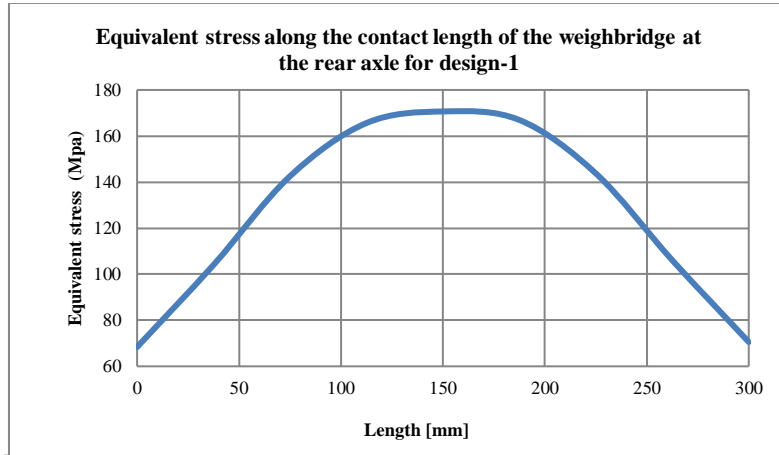


**Figure 15.** Equivalent stress along the contact length of the weighbridge at the rear axle for design-1

From the above graph it has been observed that the equivalent stress along the contact length of the weighbridge at the rear axle for design-1 increasing gradually from 68.39 MPa to 170.65 MPa and then decreasing up to 70.58 MPa as shown in figure.

**Structural Analysis of the Above-Ground Weighbridge for Design-2**

After performing structure analysis of the weighbridge for design-2 at forces of 30000 N at the front axle and 50000 N at the rear axle applied in vertical direction, the total deformation of 72.445 mm has been observed at the rear axle of the weighbridge as shown in figure.

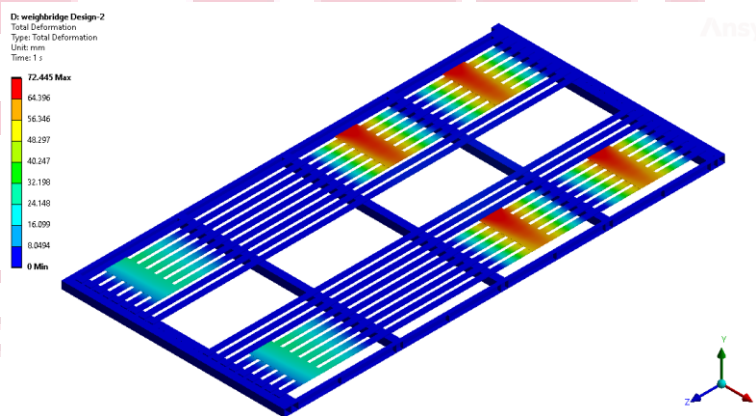


**Figure 16.** Total deformation of weighbridge for design-2

After performing structure analysis of the weighbridge for design-2 at forces of 30000 N at the front axle and 50000 N at the rear axle applied in vertical direction, the directional deformation along the Y-axis of 72.445 mm in downward direction has been observed at the rear axle of the weighbridge as shown in figure.

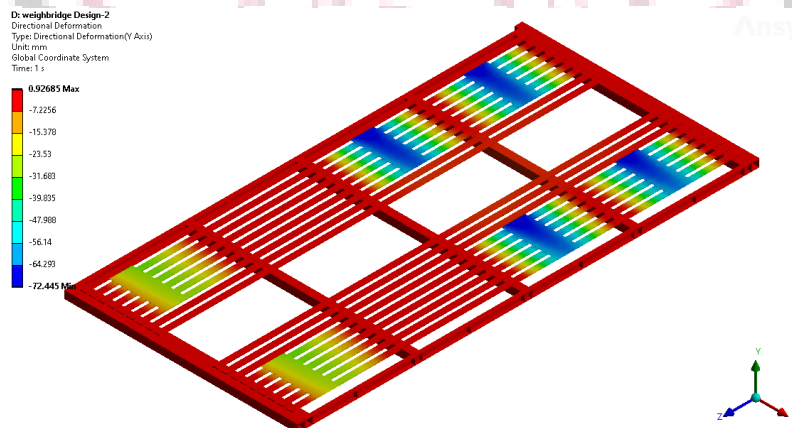


**Figure 17.** Directional deformation along Y-axis of weighbridge for design-2

After performing structure analysis of the weighbridge for design-2 at forces of 30000 N at the front axle and 50000 N at the rear axle applied in vertical direction, the maximum equivalent stress of 1093.2 MPa has been observed at the loaded portion of the rear axle of the weighbridge as shown in figure.

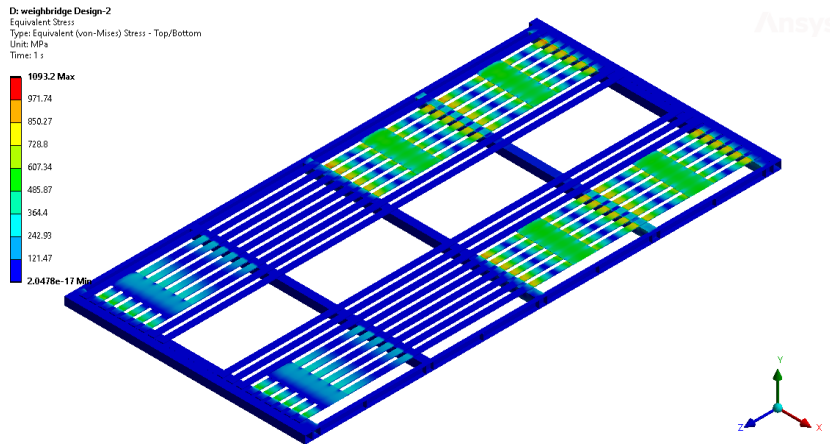


Figure 18. Equivalent stress of weighbridge for design-2

After performing structure analysis of the weighbridge for design-1 at forces of 30000 N at the front axle and 50000 N at the rear axle applied in vertical direction, the equivalent total strain of 0.00548 mm/mm (0.548%) has been observed at the loaded portion of the front & rear axle of the weighbridge as shown in figure.

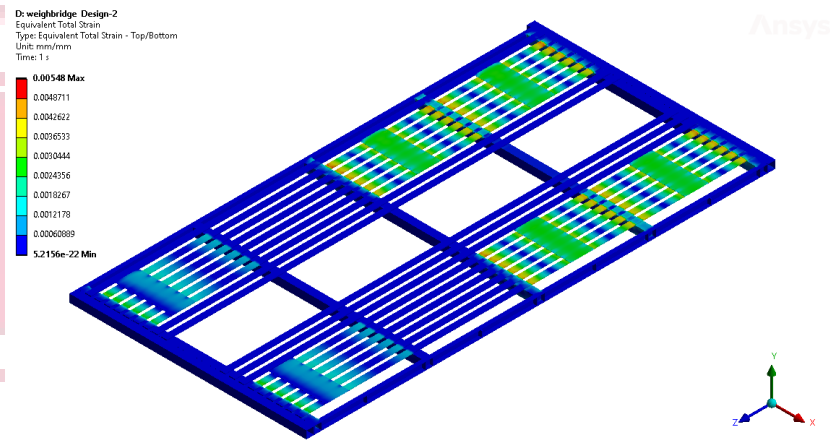


Figure 19. Equivalent strain of weighbridge for design-2

**Directional Deformation along the Contact Length of the Weighbridge at the Rear Axle for Design-2**

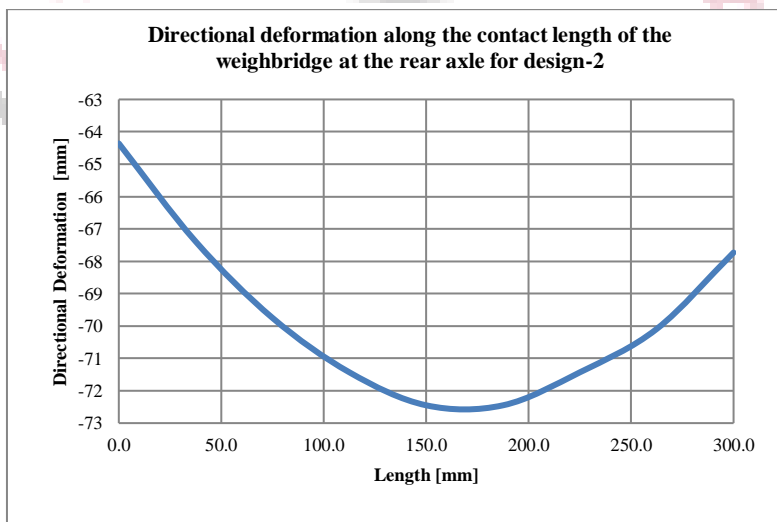
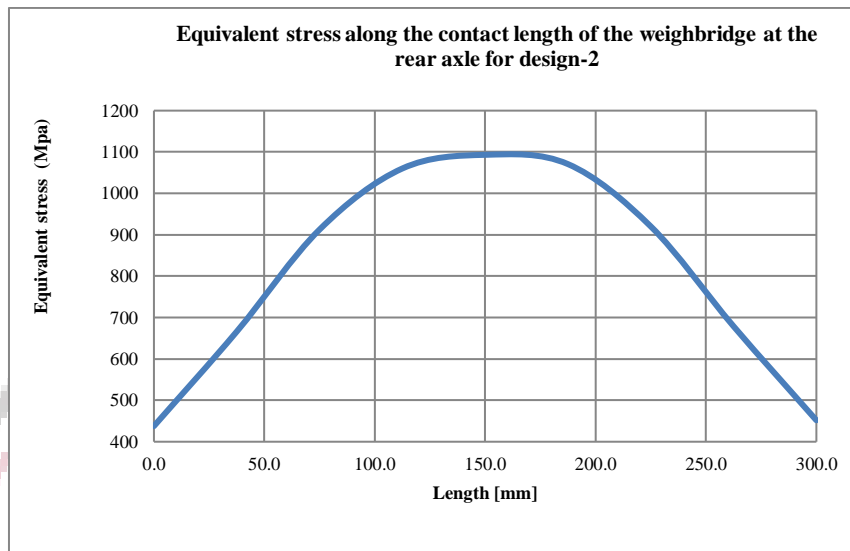


Figure 20. Directional deformation along the contact length of the weighbridge at the rear axle for design-2

From the above graph it has been observed that the Directional deformation along the contact length of the weighbridge at the rear axle for design-2 increasing gradually from 3.41 mm to 3.83 mm and then decreasing up to 3.59 mm as shown in figure.

**Equivalent Stress along the Length of the Weighbridge at the Rear Axle for Design-2**



**Figure 21.** Equivalent stress along the contact length of the weighbridge at the rear axle for design-2

From the above graph it has been observed that the equivalent stress along the contact length of the weighbridge at the rear axle for design-2 increasing gradually from 68.39 MPa to 170.65 MPa and then decreasing up to 70.58 MPa as shown in figure.

- **Structural Analysis of the Above-Ground Weighbridge for Design-3**

After performing structure analysis of the weighbridge for design-3 at forces of 30000 N at the front axle and 50000 N at the rear axle applied in vertical direction, the total deformation of 23.746 mm has been observed at the rear axle of the weighbridge as shown in figure.

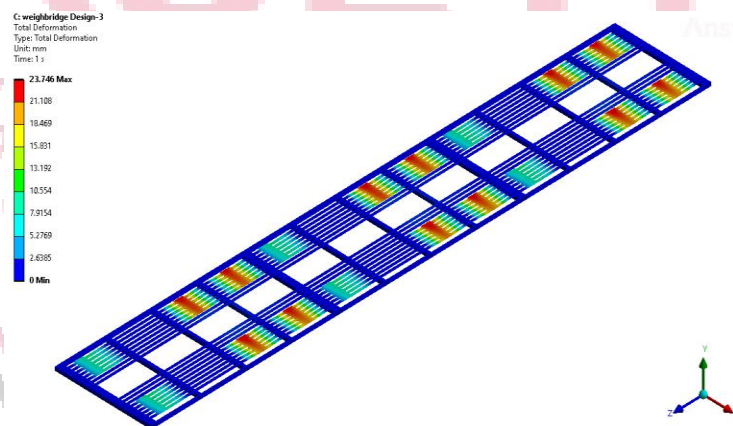


**Figure 22.** Total deformation of weighbridge for design-3

After performing structure analysis of the weighbridge for design-3 at forces of 30000 N at the front axle and 50000 N at the rear axle applied in vertical direction, the Directional deformation along the Y-axis of 23.745 mm in downward direction has been observed at the rear axle of the weighbridge as shown in figure.

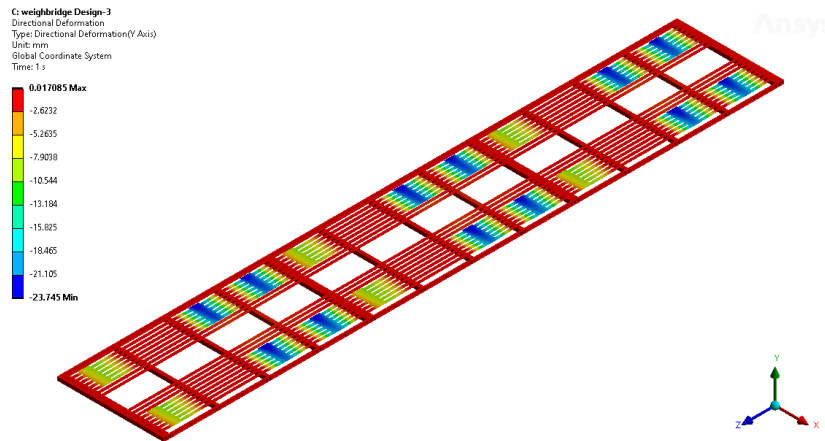


**Figure 23.** Directional deformation along Y-axis of weighbridge for design-3

After performing structure analysis of the weighbridge for design-3 at forces of 30000 N at the front axle and 50000 N at the rear axle applied in vertical direction, the maximum equivalent stress of 337.08 MPa has been observed at the loaded portion of the rear axle of the weighbridge as shown in figure.

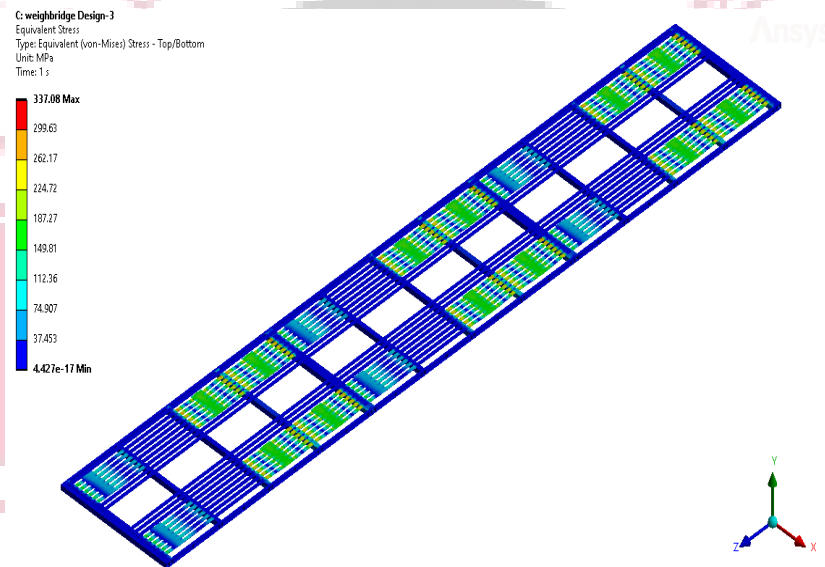


**Figure 24.** Equivalent stress of weighbridge for design-3

After performing structure analysis of the weighbridge for design-3 at forces of 30000 N at the front axle and 50000 N at the rear axle applied in vertical direction, the equivalent total strain of 0.00169 mm/mm (0.169%) has been observed at the loaded portion of the front & rear axle of the weighbridge as shown in figure.

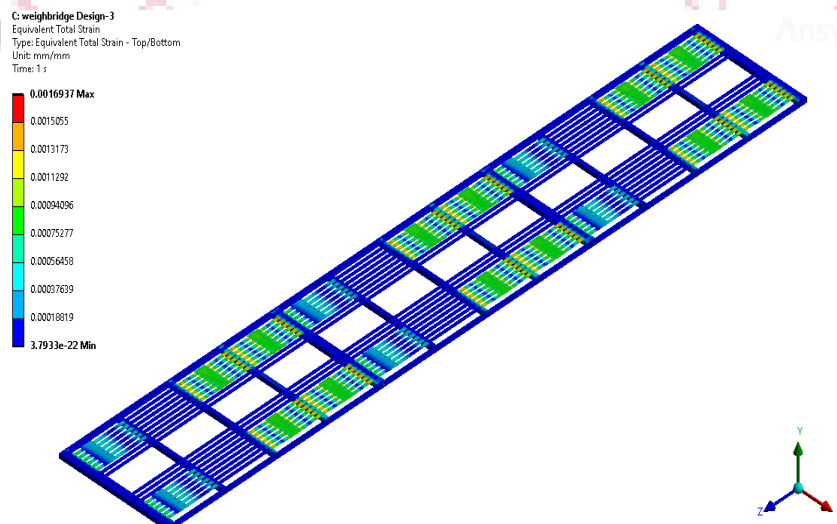


**Figure 2.5** Equivalent strain of weighbridge for design-3

**Directional Deformation along the Contact Length of the Weighbridge at the Rear Axle for Design-3**

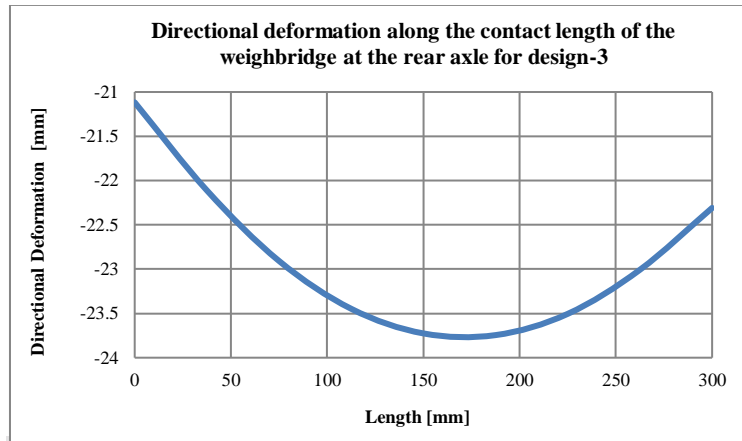


**Figure 26.** Directional deformation along the contact length of the weighbridge at the rear axle for design-3

From the above graph it has been observed that the Directional deformation along the contact length of the weighbridge at the rear axle for design-3 increasing gradually from 21.117 mm to 23.745 mm and then decreasing up to 22.309 mm as shown in figure.

**Equivalent Stress along the Length of the Weighbridge at the Rear Axle for Design-3**

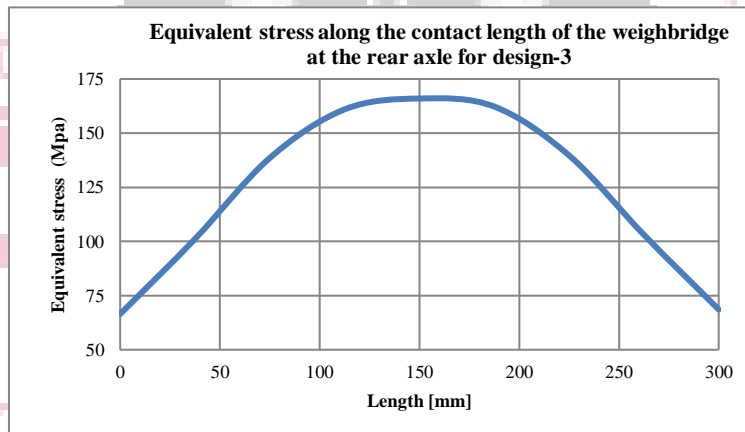


**Figure 27.** Equivalent stress along the contact length of the weighbridge at the rear axle for design-3

From the above graph it has been observed that the equivalent stress along the contact length of the weighbridge at the rear axle for design-3 increasing gradually from 66.464 MPa to 165.97 MPa and then decreasing up to 68.588 MPa as shown in figure.

**• Structural Analysis of the Above-Ground Weighbridge for Design-4.**

After performing structure analysis of the weighbridge for design-4 at forces of 30000 N at the front axle and 50000 N at the rear axle applied in vertical direction, the total deformation of 2.145 mm has been observed at the rear axle of the weighbridge as shown in figure.

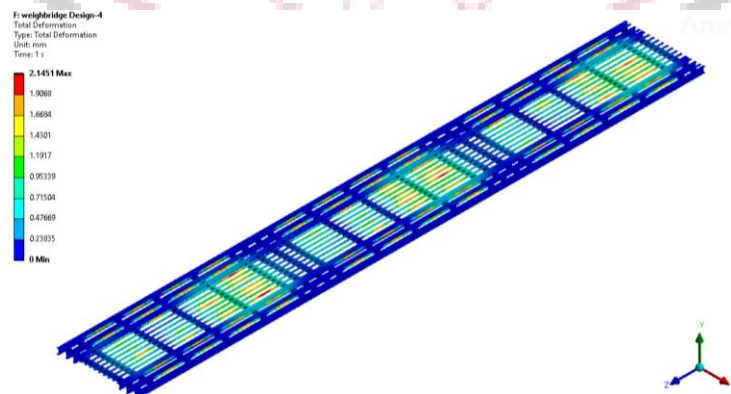


**Figure 28.** Total deformation of weighbridge for design-4



After performing structure analysis of the weighbridge for design-4 at forces of 30000 N at the front axle and 50000 N at the rear axle applied in vertical direction, the Directional deformation along the Y-axis of 2.144 mm in downward direction has been observed at the rear axle of the weighbridge as shown in figure.

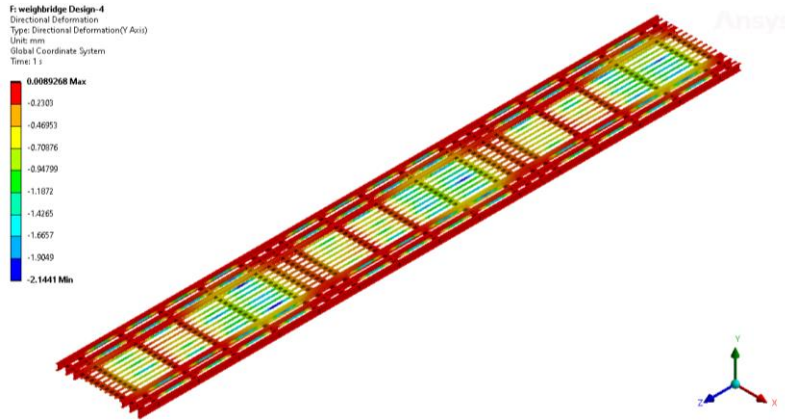


**Figure 29.** Directional deformation along Y-axis of weighbridge for design-4

After performing structure analysis of the weighbridge for design-4 at forces of 30000 N at the front axle and 50000 N at the rear axle applied in vertical direction, the maximum equivalent stress of 50.723 MPa has been observed at the loaded portion of the rear axle of the weighbridge as shown in figure.

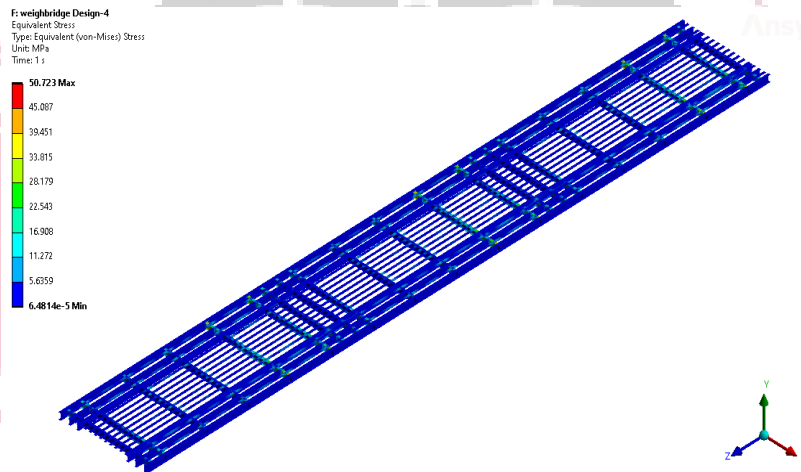


**Figure 30.** Equivalent stress of weighbridge for design-4

After performing structure analysis of the weighbridge for design-4 at forces of 30000 N at the front axle and 50000 N at the rear axle applied in vertical direction, the equivalent total strain of 0.000255 mm/mm (0.0255%) has been observed at the loaded portion of the front & rear axle of the weighbridge as shown in figure.

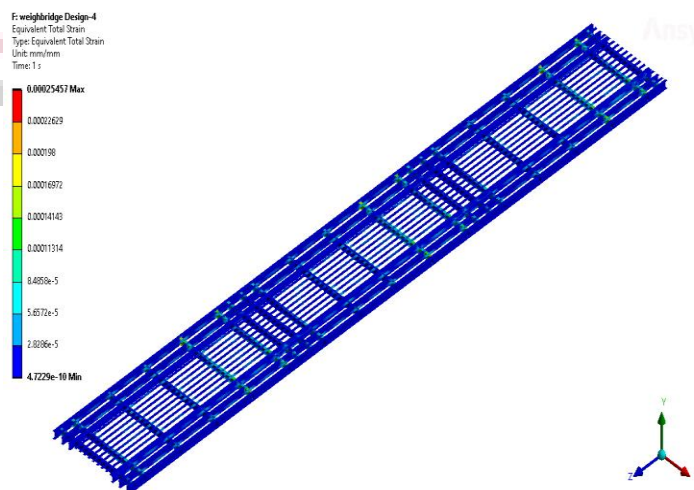


**Figure 31.** Equivalent strain of weighbridge for design-4

**Directional Deformation Along the Contact Length of the Weighbridge at the Rear Axle for Design-4**

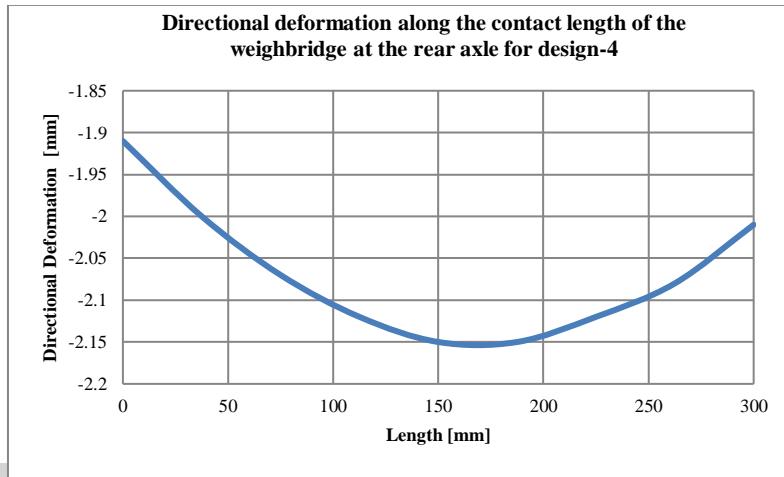


**Figure 32.** Directional deformation along the contact length of the weighbridge at the rear axle for design-4

From the above graph it has been observed that the Directional deformation along the contact length of the weighbridge at the rear axle for design-3 increasing gradually from 1.91 mm to 2.15 mm and then decreasing up to 2.01 mm as shown in figure.

**Equivalent Stress along the Contact Length of the Weighbridge at the Rear Axle for Design-4**

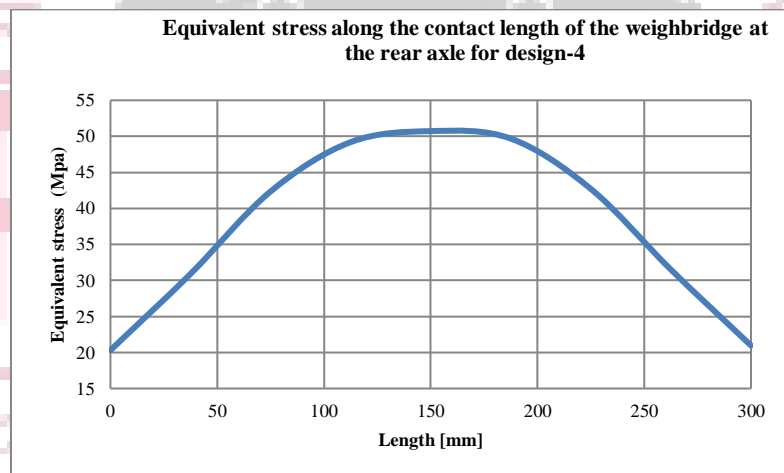


**Figure 33.** Equivalent stress along the contact length of the weighbridge at the rear axle for design-4

From the above graph, it is observed that equivalent stress along the contact length of the weighbridge at the rear axle for design-3 increasing gradually from 20.312 MPa to 50.723 MPa and then decreasing up to 20.962 MPa as shown in figure.

**B. Comparative result of Directional Deformation Along the Length of the Weighbridge at the Rear Axle**

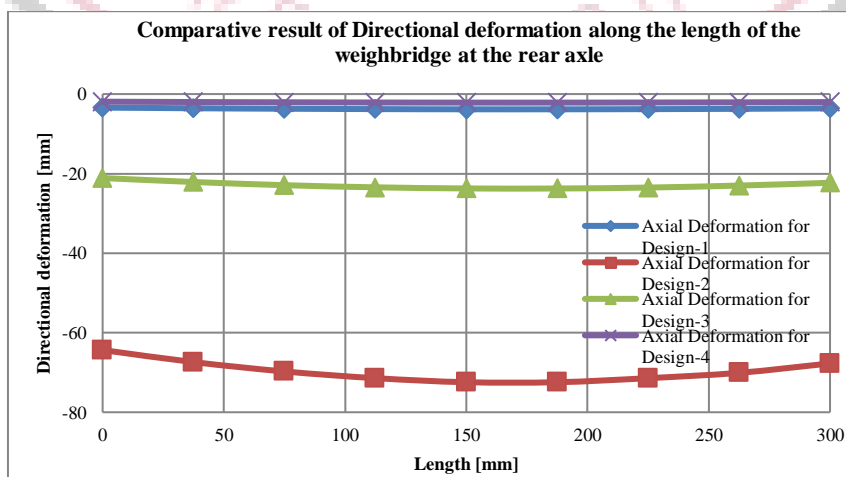


**Figure 34.** Comparative result of Directional deformation along the length of the weighbridge at the rear axle

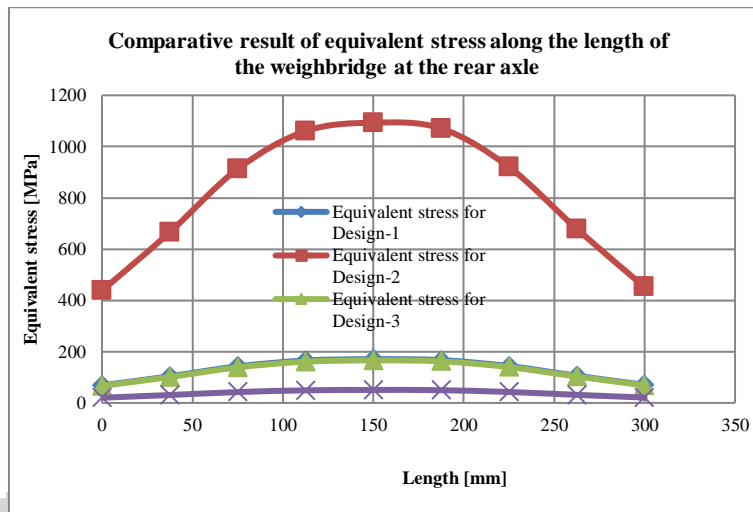


Figure 35. Comparative result of equivalent stress along the length of the weighbridge at the rear axle

C. Comparative result of Total Deformation of the Weighbridge for all Designs

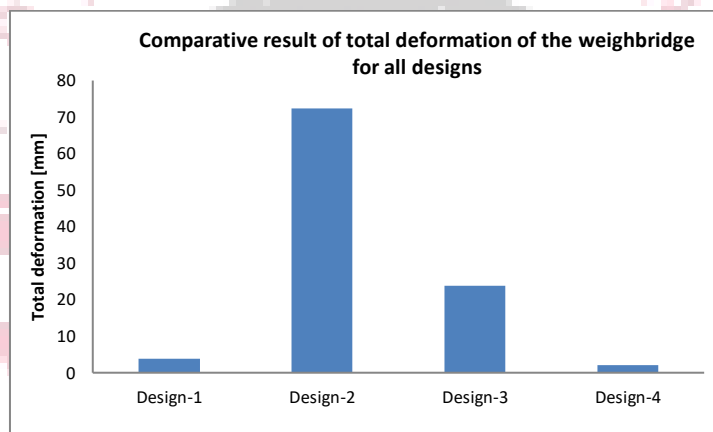


Figure 36. Comparative result of total deformation of the weighbridge for all designs

From the above graph it has been observed that the comparative result of total deformation of the weighbridge for all designs have the maximum total deformation of 72.445 mm for design-2 while the minimum deformation of 2.145 mm has been observed for design-4 as shown in figure. Hence design-4 of above-ground weighbridge has been proposed.

D. Comparative Result of Directional Deformation of the Weighbridge for all Designs

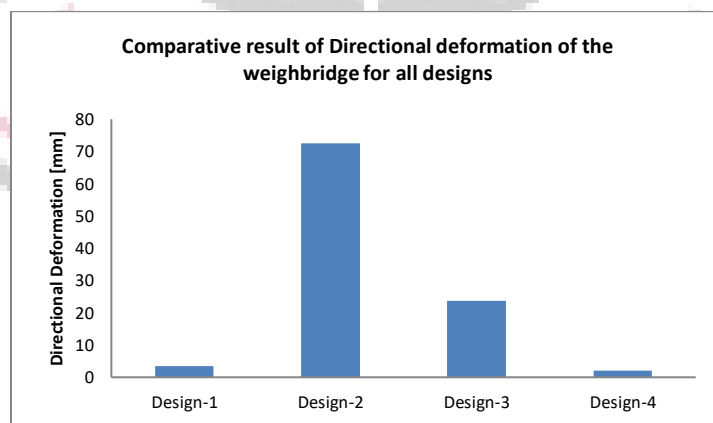
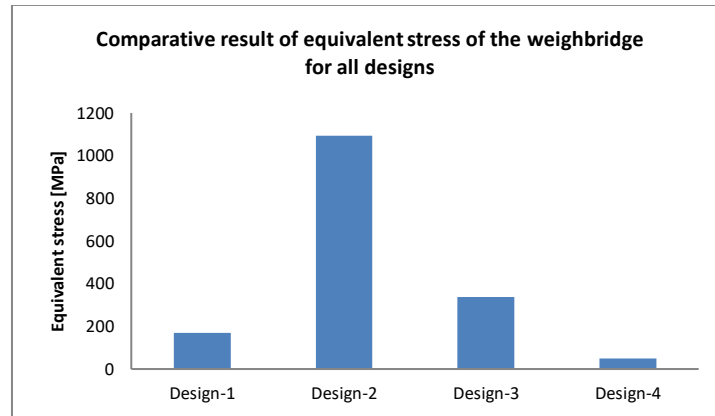


Figure 37. Comparative result of Directional deformation of the weighbridge for all designs

From the above graph it has been observed that the comparative result of Directional deformation of the weighbridge for all designs have the maximum Directional deformation of 72.445 mm for design-2 while the minimum deformation of 2.144 mm has been observed for design-4 as shown in figure. Hence design-4 of above-ground weighbridge has been proposed.

### E. Comparative Result of Equivalent Stress of the Weighbridge for all Designs



**Figure 38.** Comparative result of equivalent stress of the weighbridge for all designs

From the above graph it has been observed that the comparative result of equivalent stress of the weighbridge for all designs have the maximum stress of 1093.2 MPa for design-2 while the minimum deformation of 50.723 MPa has been observed for design-4 as shown in figure. Hence design-4 of above-ground weighbridge has been proposed.

### F. Comparative Result of Equivalent Strain or Permanent Deformation of the Weighbridge for all Designs

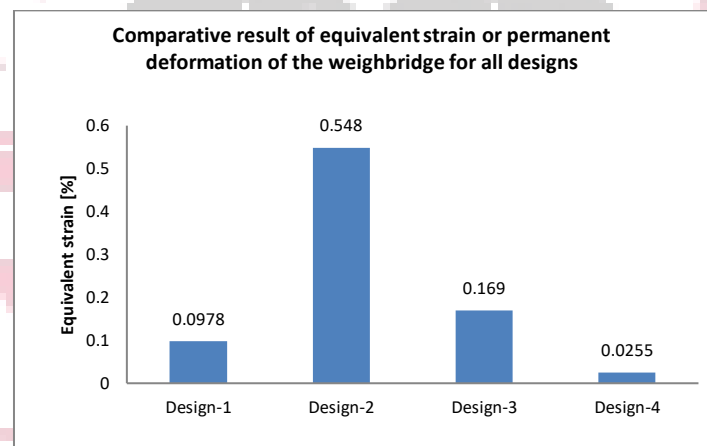


**Figure 39.** Comparative result of equivalent strain or permanent deformation of the weighbridge for all designs

From the above graph it has been observed that the comparative result of equivalent strain or permanent deformation of the weighbridge for all designs have the maximum permanent deformation of 0.548% for design-2 while the minimum permanent deformation of 0.0255% has been observed for design-4 as shown in figure. Hence design-4 of above-ground weighbridge has been proposed.

## V. CONCLUSION

This study underscores the crucial role of weighbridges in addressing vehicle overloading and preserving road pavement. The cost-effectiveness of weighbridges is influenced by various external factors and operational expenses. The working principle of weighbridges using load cells and strain gauges has been explained. The advantages of weighbridge utilization, including productivity enhancement and compliance enforcement, have been highlighted. The primary focus of the study was on designing and optimizing an above-ground weighbridge using finite element analysis. Structural analyses of four proposed designs were conducted, considering deformation, stress, and equivalent strain. The comparative results suggest that design-4 offers the most optimal performance in terms of permanent deformation. This research contributes to the field of transportation infrastructure management by providing insights into weighbridge functionality, design optimization, and the cost-effective management of vehicle loads.

## REFERENCES

- [1] Miss. P.B. Ramteke et al. (2015). "Design, Modeling and Fem Analysis of Weighbridge" IJSRD - International Journal for Scientific Research & Development| Vol. 3, Issue 05, 2015 | ISSN (online): 2321-0611; <https://www.ijsrd.com/articles/IJSRDV3I50222>.
- [2] <https://coalhandlingplants.com/weighbridge-truck-scale/>

- [3] <https://weigh-more.com.au/commercial-applications-and-benefits-of-weighbridges/>
- [4] Li, J., et al. (2020). "Coupled CFD-DEM analysis of parameters on bridging in the fracture during lost circulation." *Journal of Petroleum Science and Engineering*, 184, 106501. doi:10.1016/j.petrol.2019.106501.
- [5] Shu, J., et al. (2019). "Assessment of a cantilever bridge deck slab using multi-level assessment strategy and decision support framework." *Engineering Structures*, 200, 109666. doi:10.1016/j.engstruct.2019.109666.
- [6] Hassoun, M., & Fatahi, B. (2019). "Novel integrated ground anchor technology for the seismic protection of isolated segmented cantilever bridges." *Soil Dynamics and Earthquake Engineering*, 125, 105709. doi:10.1016/j.soildyn.2019.105709.
- [7] Mokrani, B., et al. (2017). "Passive damping of suspension bridges using multi-degree of freedom tuned mass dampers." *Engineering Structures*, 153, 749–756. doi:10.1016/j.engstruct.2017.10.028.
- [8] Cantero, D., et al. (2017). "Evolution of bridge frequencies and modes of vibration during truck passage." *Engineering Structures*, 152, 452–464. doi:10.1016/j.engstruct.2017.09.039.
- [9] Bistak, M., et al. (2017). "The Above-ground Weighbridge." *Procedia Engineering*, 192, 52–57. doi:10.1016/j.proeng.2017.06.009.

